



Membrane-type metamaterials: Transmission loss of multi-celled arrays

Yi-Jen Huang, Chia-Hao Wang, Yu-Lin Huang, Gangjian Guo, Steven R. Nutt

Department of Chemical Engineering and Materials Science, M.C. Gill Composites Center, University of Southern California, Los Angeles, California 90089-010

Abstract: Composite syntactic foams with different densities were fabricated with hollow phenolic microspheres, a phenolic resin binder, and a small addition of chopped carbon fibers. Compressive, shear, and tensile proper-ties were studied for the syntactic foams with and without carbon fibers. Two fiber layer orientations, either parallel (P-type) or perpendicular (N-type) to the loading direction, were considered in the mechanical testing. For N-type foams, mechanical properties were weakly dependent on foam density. For P-type foams, the mechanical properties of the foams were strongly dependent on the strength of the supporting matrix. The specific strength and specific stiffness of the P-type foams were significantly enhanced compared with the neat foams. These findings indicate that fiber reinforcement is an effective way to enhance the mechanical performance of syntactic foams, and the enhanced performance should lead to applications as a foam core material for sandwich structures.

1. Introduction

Syntactic foams are ultra-lightweight materials com-prised of hollow microspheres (filler) and a resinous matrix (binder) [1]. The micro spheres (or micro balloons) can consist of inorganic materials, such as glass and silica, or polymeric materials, such as epoxy, unsaturated polyester, phenolics, and polyvinyl chloride [2 (p. 489)]. The binder is typically a thermosetting resin, such as epoxy, phenolic, or polyester [3, 4]. Compared with conventional foams, syntactic foams generally

Please cite this article as: Yi-Jen Huang, Chia-Hao Wang, Yu-Lin Huang, Gangjian Guo, and S.R. Nutt, **Enhancing the specific strength and specific stiffness of phenolic microsphere syntactic foams reinforced with carbon fibers**, *Polymer Compos*, 31 [2] (2009) 256-262, DOI:<http://dx.doi.org/10.1002/pc.20795>



offer superior specific compressive strength and lower moisture absorption due to the closed-cell structure. However, despite the superior compressive strength of syntactic foams, the tensile and shear strengths generally are inferior to conventional foams. They are widely used in marine applications as a buoyancy material and in structural applications as a foam core material for sandwich panels [2 (p 355), 5–9]. Syntactic foams can be classified as either a two-phase system containing negligible entrapped air bubbles in the resinous matrix (e.g., by vacuum manufacturing), or a three-phase system in which air bubbles are included [4]. The interstitial void space in the three-phase syntactic foams sometimes is intentionally introduced by using a limited amount of binding material, for the purpose of lowering the foam density.

The mechanical properties of syntactic foams can be tailored by using different types of binders and/or micro-spheres, modifying the interface between the matrix and the microspheres, and modulating the overall foam density [10–12]. For example, the increase of wall thickness of micro ballons of the same outer diameter reportedly increases the compressive strength [13]. Wouterson et al. blended glass and phenolic microspheres with an epoxy resin (the binder) [14] and showed that the mechanical properties were dependent on the properties and proportions of both types of microspheres. Kishore et al. investigated the effects of interface modification on the strength and fractographic features of syntactic foam slabs, and concluded that the paraffin oil coated micro ballons led to the reduced strength due to the weakened interface between the microballons and the matrix [15]. Despite the superior compressive strength of syntactic foams, the tensile and shear strengths generally are inferior to conventional foams. Gutpa et al. demonstrated that a typical glass microsphere-based syntactic foam with a density of 600 kg/m^3 showed a compressive strength of 66 MPa, whereas the tensile strength and shear strength were only 23 and 26 MPa, respectively [16].



Observations of fracture surfaces from tensile and shear tests reveal that failures are primarily interfacial or matrix-dominated, limiting the strengths [1].

Fiber reinforcement can also be used to strengthen and stiffen syntactic foams. For example, Karthikeyan et al. added 3 wt% of 6 mm glass fibers to the syntactic foam based on glass microsphere, improving the flexural strength by 30% [3]. The compressive strength increased by 15–20% with the addition of up to 5% fibers [17]. However, Gupta et al. found that the addition of fibers led to increased interstitial voids, and therefore the strength decreased when compared with the neat syntactic foam [6, 18]. Karthikeyan et al. further used ultrasonic imaging to detect the void content in the syntactic foam and concluded that the higher void content was responsible for the lower compression strength [19]. To reduce the void content, Gupta et al. [18] modified the synthesis process, greatly reducing the void content and enhancing the strength.

Table 1: Properties of carbon (C-30) fibers.

Sample	Density (kg/m ³)	Fiber diameter (μm)	Tensile modulus (GPa)	Tensile strength (GPa)
C-30	1,810	7	225	3.5

Glass microspheres are most commonly used as fillers in syntactic foams. However, they are stiff and brittle, which influences foam performance and limits applications. In contrast, syntactic foams based on polymeric microspheres generally are tougher and less brittle and can offer other advantages such as enhanced machinability, improved compatibility with resins, etc. [20]. Such foams can be strengthened and stiffened by fiber reinforcement to achieve performance competitive with other foam core materials used in sandwich panels. Our previous study [21] demonstrated the enhanced properties (i.e., compression, shear, tensile) of amino microsphere-based syntactic foams reinforced with chopped carbon fibers and aramid fibers.



This study was undertaken to synthesize the phenolic microsphere-based syntactic foams reinforced with a small addition of chopped carbon fibers and to investigate their mechanical properties. Particularly, the aim of this study was to focus on enhancing the specific strength and specific stiffness of the composite foam. Composite foams with different densities and fiber orientations were produced, and the relations between the foam density and the mechanical properties, including compression, tension, and shear, were determined. This study illustrates an approach to produce composite syntactic foams with superior specific strength.

2. Experimental

2.1 Materials

Hollow phenolic microspheres (PHENOSET1BJO-0930 Asia Pacific Microspheres Corp.) were used to fabricate syntactic foams with different fiber loadings. The phenolic microspheres are typically used as fillers in polymer composites and in adhesives to reduce density and to enhance flame retardancy and compressive strength. The microsphere mean diameter was 70 μm , the true density was 210–250 kg/m^3 , and the hydrostatic compressive strength was 3.4 MPa [22]. Phenolic resol resin (Schenec-tady International, Inc.) was chosen as the polymer binder. Carbon fiber (C-30, SGL Carbon AG) was selected as the reinforcement and the average length was ~ 12 mm. Properties of C-30 fibers are presented in Table1 [23].

2.2 Synthesis of Fiber Reinforced Syntactic Foams

The microstructure of the typical syntactic foams consisted of microspheres, resin, and voids, as shown in Fig.1. Voids are included to obtain low-density foams while retaining high strength. In the



fiber-reinforced samples, the carbon fibers span thousands of microspheres. In this study, all fiber-reinforced foams were fabricated with a composition of 4 wt% fiber, 19 wt% phenolic resin, and 77 wt% phenolic microspheres. The syntactic foams were synthesized with three densities: 250, 300, and 350 kg/m³. Preforms were made by first immersing fibers and microspheres in a 5 wt% solution of phenolic resin in ethyl alcohol and mixing. Next, preforms were dried for 24 h at 208C, followed by hot compaction and curing for 40 min at 1508C. The six preforms were stacked with parallel fiber layers before the compaction step. The compaction pressure was just sufficient to achieve the desired sample volume (and density). The fibers were randomly oriented within the plane normal to the compaction direction. Neat syntactic foams were fabricated as a control material using the same processing conditions, and they consisted of 23 wt% phenolic resin and 77 wt% phenolic microspheres.

2.3 Mechanical Properties

Compressive, shear, and tensile tests were performed on composite syntactic foams in accordance with ASTM standards D 1621 – 73, C – 273, D 1623 – 78, respectively. The specimen dimensions for both compressive and tensile testing were 25.4 × 25.4 × 25.4 mm³, whereas shear specimens were 25.4 × 25.4 × 6.2 mm³. Two fiber plane orientations were used in testing. In the first orientation, designated as N, the XY-fiber plane was perpendicular (normal) to the load axis, as shown in Fig.2, whereas in the second orientation, designated as P, the sample was turned 90°, with the fiber plane parallel to the load axis, as shown in Fig. 2. At least five samples were tested for each material condition. Samples were examined before and after testing with a light microscope.

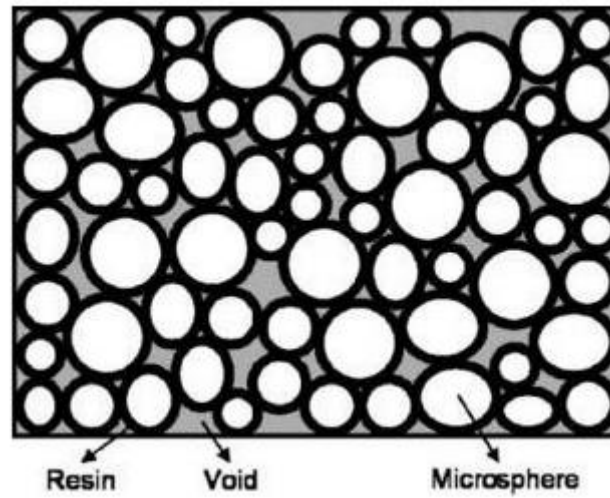


Figure 1: Schematic morphology of typical syntactic foam.

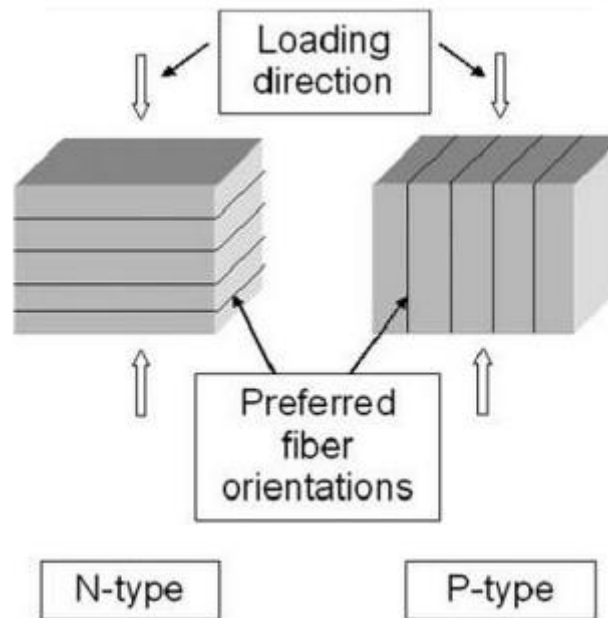


Figure 2: Definition of N-type and P-type foams.



3. Results and Discussion

3.1 Compression

Compressive tests were conducted on the neat foam sand fiber-reinforced foams, and the influence of foam density and fiber preferred orientation was analysed. The compressive strength and modulus values for the foam samples are summarized in Table 2. For all foams, both the compressive strength and modulus increased with an increase in foam density, as expected. Compared with the neat foams, the compressive properties of P-type composite foams increased significantly. However, the N-type foams showed yield strength and modulus values similar to the neat foams. The neat foam was tested in both the compaction direction and 90° to the compaction direction and no significant change in the strength values was observed. Often, foam properties obey a simplified power law [24]:

$$A(\rho) = A_0\rho^n \quad (1)$$

where A is a foam property, ρ is the foam density, A_0 is a factor which reflects the properties of the solid cell wall materials, and n is an exponent. By fitting the compressive modulus data to the power law, the exponent values determined are 1.01, 1.83, and 1.58 for the P-type foam, the neat foam, and the N-type foam, respectively. The corresponding correlation factors are 1, 0.99, and 0.89, respectively.

The compressive modulus of fiber-reinforced syntactic foams exhibit the expected power law behavior, although fiber orientation strongly affects the exponent in the density range studied. The compressive stress–strain curves for the syntactic foams (density = 300 kg/m³) are shown in Fig. 3.

The curves illustrate the different failure behavior of the fiber-reinforced foams and the influence of fiber orientation. Both the neat foam and the N-type composite foams showed a monotonically



increasing stress caused by compaction of voids after yielding [5]. However, when the strain exceeded 20%, the compressive stress of the neat foam dropped, a consequence of fractures at sample corners and edges, as shown in Fig. 4. In neat foams, fracture occurs along a plane inclined 45° to the load axis. Voids within the samples diminish the compressive strength because of stress concentrations at void tips. Cracks initiate at these sites and propagate either along microsphere surfaces or through the microspheres. To clarify the fracture mechanism of the neat foam, fracture surfaces were examined by scanning electron microscope (SEM) (Fig. 5). Most micro spheres fractured after the compressive test and provided evidence that cracks propagated through the microspheres.

Figure 4 shows that the N-type foam retained shape and that cracks propagated within the fiber layer plane, approximately normal to the stress axis. For N-type foams, failure occurred parallel to the fiber layer planes, which are defined in Fig. 2. Introducing the fiber layers led to additional voids between the fiber layer planes and the matrix, increasing the local void fraction at interfacial areas between the fiber layer and the matrix. This can be explained by the interlacing of the fibers, as shown in Fig. 6. The SEM image shows interstitial spaces devoid of micro spheres that are created by fiber intersections. These interstitial void spaces were the weakest parts of the N-type foams, severely limiting the compressive strength. Thus, the compressive strength of N-type foams was limited by the interfacial strength between the fiber layer planes and the matrix instead of the matrix strength.

Table 2: Compression test.

Sample	$D = 250 \text{ kg/m}^3$		$D = 300 \text{ kg/m}^3$		$D = 350 \text{ kg/m}^3$	
	Stress (MPa)	Modulus (MPa)	Stress (MPa)	Modulus (MPa)	Stress (MPa)	Modulus (MPa)
Neat	1.87 ± 0.12	65 ± 5	2.83 ± 0.25	93 ± 6	4.55 ± 0.31	120 ± 11
N-type	2.06 ± 0.18	70 ± 5	3.16 ± 0.26	89 ± 7	4.05 ± 0.27	120 ± 10
P-type	4.80 ± 0.34	216 ± 19	6.27 ± 0.57	259 ± 23	8.33 ± 0.65	303 ± 27

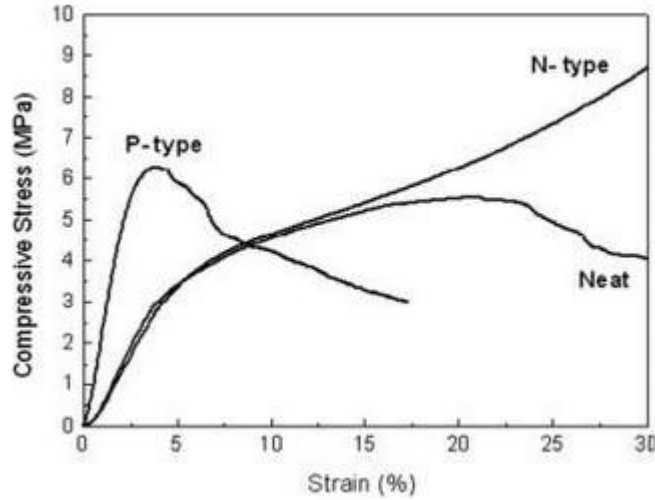


Figure 3: Compressive stress–strain curves for syntactic foams (density = 300 kg/m³).

A different failure mode was observed for the P-type foam, shown in Fig. 3. The compressive stress decreased sharply after reaching a peak stress. This behavior was caused by separation between the fibers and the supporting matrix. For the P-type foam, cracks propagated initially along the 45° plane, and then deflected along the preferred fiber orientation. The separation (or debonding) resulted from transverse tensile forces in the lateral direction due to the Poisson's effect. Once such separation occurs, the matrix cannot transfer load to the fibers and the resistance to the compressive load drops. The steeper slope of the P-type loading curve indicates a substantial enhancement in compressive modulus. This can be attributed to the stiffness of the carbon fibers and the supporting foam cells [25].

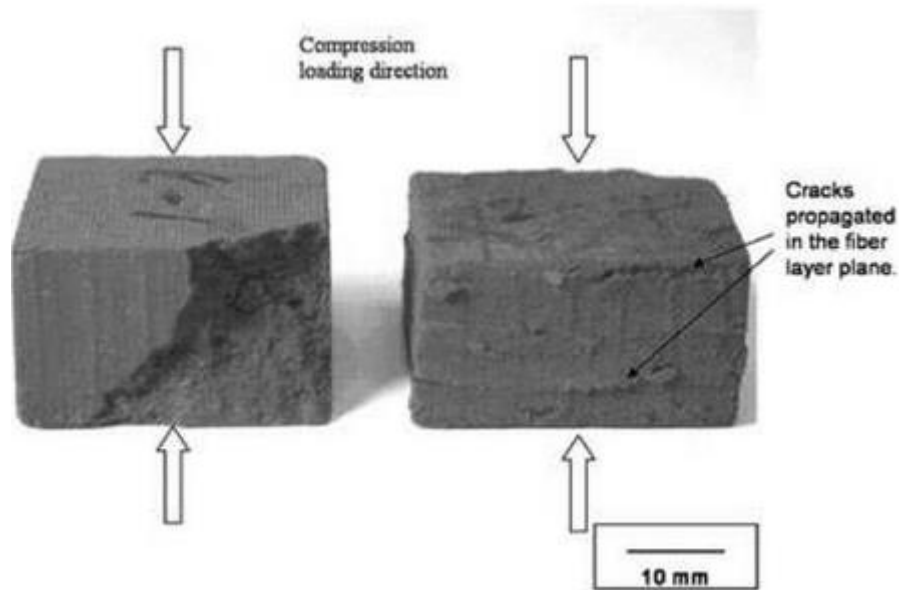


Figure 4: Neat (left) and N-type (right) foams after compression test. N-type foams represent the fiber reinforced foams with the XY fiber plane perpendicular (normal) to the load axis.

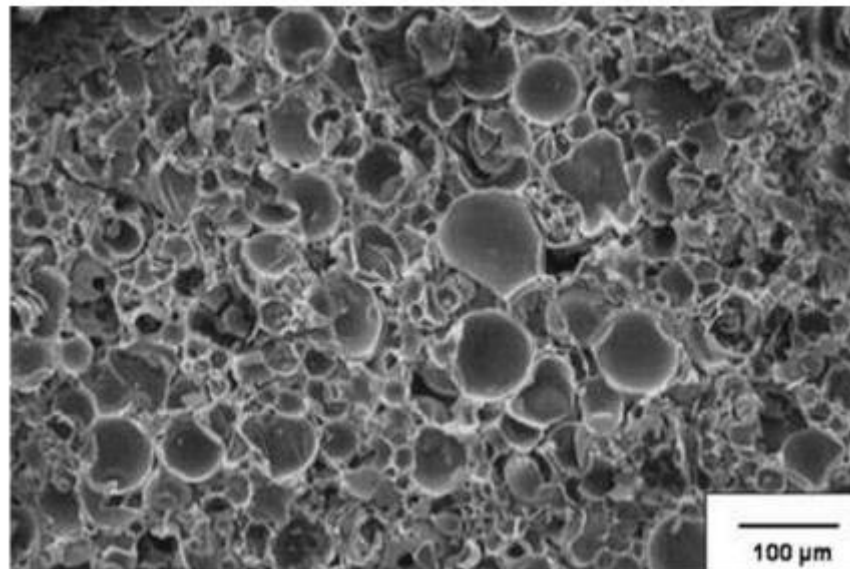


Figure 5: SEM image of the neat foam (density = 300 kg/m³)



3.2 Tension

The tensile strength and modulus values for foam samples are summarized in Table 3. For the neat and P-type foams, both tensile strength and modulus increased with increasing foam density. However, for N-type foams, the tensile strength was insignificantly dependent on foam density. For neat foams, increasing density from 250 kg/m³ to 350 kg/m³ resulted in increases in tensile strength and modulus of 36% and 31%, respectively. For P-type foams, increasing density from 250 kg/m³ to 350 kg/m³ resulted in an increase of 210% in both tensile stress and modulus. The tensile strength values for all N-type foams were ~1 MPa, although the tensile modulus increased from 120 MPa to 160 MPa when the foam density increased from 250 kg/m³ to 350 kg/m³.

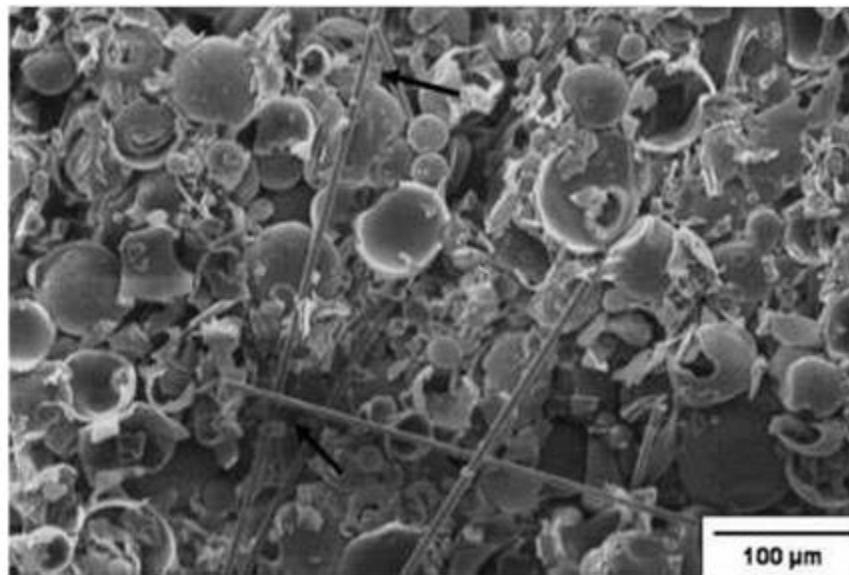


Figure 6: SEM image of the N-type foam (density = 300 kg/m³).



Table 3: Tensile test.

Sample	$D = 250 \text{ kg/m}^3$		$D = 300 \text{ kg/m}^3$		$D = 350 \text{ kg/m}^3$	
	Stress (MPa)	Modulus (MPa)	Stress (MPa)	Modulus (MPa)	Stress (MPa)	Modulus (MPa)
Neat	1.33 ± 0.11	140 ± 12	1.64 ± 0.13	160 ± 14	1.95 ± 0.16	184 ± 11
N-type	1.01 ± 0.09	120 ± 11	1.06 ± 0.08	150 ± 13	1.18 ± 0.07	160 ± 14
P-type	1.76 ± 0.12	188 ± 13	2.71 ± 0.22	262 ± 22	3.72 ± 0.22	395 ± 31

For the neat foam, fracture occurred in the middle of the gage section. SEM examination of the fracture surface revealed that fracture propagated through the micro-spheres. The key factor controlling the tensile strength and modulus of the neat foam is the volume fraction of voids. Luxmoore and Owen [26] concluded that a crack will initiate from an oversized void when a composite is subjected to tensile loading. Therefore, as foam density is increased, strength and modulus are expected to increase. For the N-type foam, foam failure occurred along the preferred fiber plane, normal to the load axis. Fracture occurred at sites where the local volume fraction of voids was greatest, just as in the case of compression loading. The strength and stiffness of N-type foams were insensitive to foam density.

For P-type foams, failure involved two components: first, the failure of the matrix and second, pull out of the fibers. After matrix failure, carbon fibers bridged foam cracks and resisted crack opening. The primary factor controlling failure initiation was matrix failure. For P-type foams, fibers carry much of the applied load, leading to tensile strength 30–90% greater than the neat foams of comparable density. Likewise, tensile modulus values were 34%, 63%, and 114% greater for P-type foams of three different densities, reflecting fiber-dominated behavior. Also, the denser matrix provided better support to the fibers and resulted in better reinforcement.

Tensile stress–strain curves for composite syntactic foams are shown in Fig. 7. The curves illustrate different failure behavior of the P-type foam compared with the neat and the N-type foams. Both the neat and the N-type composite foams exhibit brittle fracture after yielding, while the P-type foams



carry substantial loads long after yielding. The post yield behavior derives from crack bridging and fiber pullout, processes which boost fracture toughness. In contrast, fiber orientations in N-type foams do little to enhance the load-carrying capacity of the composite foam, and these foams behave much like neat foams.

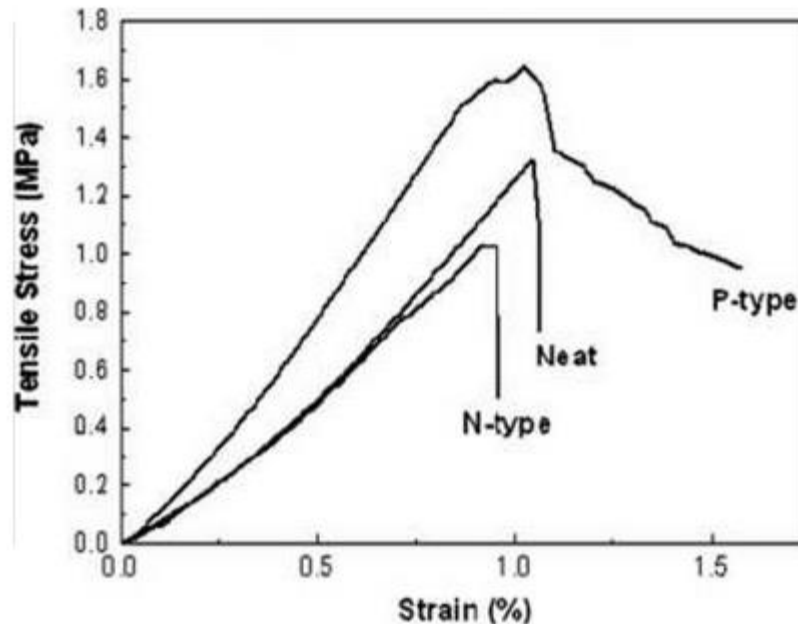


Figure 7: Tensile stress-strain curves for syntactic foams (density = 250kg/m³).

3.3 Shear

The shear strength and modulus values for foam samples are summarized in Table 4. For neat foams, the shear strength and modulus increased slightly with increasing foam density. When density was increased from 250 kg/m³ to 350 kg/m³, the shear stress and modulus increased 3% and 44%, respectively. Similarly, for P-type fiber-reinforced foams, shear strength and modulus increased 22% and 20%, respectively, with increasing density. However, when compared with the neat foam, the P-type foam (350 kg/m³ density) showed 150% and 102% increases in shear strength and modulus,



respectively. N-type foams showed insignificant density dependence on both shears trength and modulus. However, when compared to neat foam, the N-type foams showed 60% increase in shear strength, although the shear modulus was similar to the neat foams at all foam densities.

The shear properties of the neat and the N-type foams do not show a strong dependence on density, unlike the tensile and compressive properties. In the neat foam, cracks propagate primarily through the interfaces between adjoining micro spheres. In this case, the shear strength and also shear modulus are determined primarily by the shear properties of resin binder. In the N-type foam, cracks propagate in planes parallel to the preferred fiber plane. Therefore, shear strength and modulus are largely controlled by the local volume fraction of voids rather than the global density of the matrix. After shear testing, the surface of the N-type foam was fibrous and brush-like, indicating extensive fiber pullout. The process of fiber pullout absorbs energy [27] and contributes to their creased shear strength of the N-type foam. In P-type foams, interlaced fibers resists shear loads and shear fracture, enhancing shear strength. The interlacing of fibers leads to the enhanced shear performance of the foam.

Typical shear stress–strain curves for the syntactic foams are shown in Fig. 8. All curves illustrate brittle behavior after peak stress. Moduli of the N-type foam tend to be similar to the neat foam, whereas P-type foams show enhanced modulus. This phenomenon is attributed to the larger number of voids introduced by the fiber layer planes for the N-type foams, which weaken the resistance to shear loads.

Table 4: Shear test.

Sample	$D = 250 \text{ kg/m}^3$		$D = 300 \text{ kg/m}^3$		$D = 350 \text{ kg/m}^3$	
	Stress (MPa)	Modulus (MPa)	Stress (MPa)	Modulus (MPa)	Stress (MPa)	Modulus (MPa)
Neat	2.32 ± 0.19	25 ± 2	2.35 ± 0.21	29 ± 3	2.38 ± 0.21	36 ± 4
N-type	3.81 ± 0.28	31 ± 2	3.84 ± 0.34	31 ± 4	3.85 ± 0.33	31 ± 3
P-type	4.85 ± 0.39	61 ± 5	5.34 ± 0.48	63 ± 6	5.94 ± 0.47	73 ± 8



3.4 Specific Strength and Specific Stiffness

The specific strength and specific stiffness for the P-type foams and the neat foams are shown in Fig. 9. The specific strength is known as the strength-to-weight ratio and the specific stiffness is known as the stiffness-to-weight ratio. Compared with the neat foams, P-type foams displayed a much higher specific strength and stiffness in compression, tension, and shear. P-type foams (350 kg/m^3) exhibited the greatest specific strength and specific stiffness in compression and tension, whereas P-type foams (250 kg/m^3) showed the greatest specific strength and stiffness in shear. When the density of P-type foams was increased 40%, the specific shear strength and specific shear modulus actually decreased by 22% and 20%, (unlike the specific tensile and compressive strengths). However, the density dependence of the specific shear strength and shear modulus was relatively weak for all foam types, and again it is because shear strength and modulus are largely controlled by the local volume fraction of voids rather than the global density of the matrix. The specific compressive strength and the specific tensile strength increased with increasing composite foam density. However, the specific shear strength decreased with increasing composite foam density, as shown in Fig. 9a. Wouterson et al. reinforced the epoxy resin with phenolic microspheres, and concluded that the specific compressive stiffness leveled off as the increase in stiffness was counter balanced by the increased density of the composite [14]. A similar phenomenon occurred in the present work, where the specific stiffness for compressive and shear loading was essentially independent of foam density, as shown in Fig. 9b.

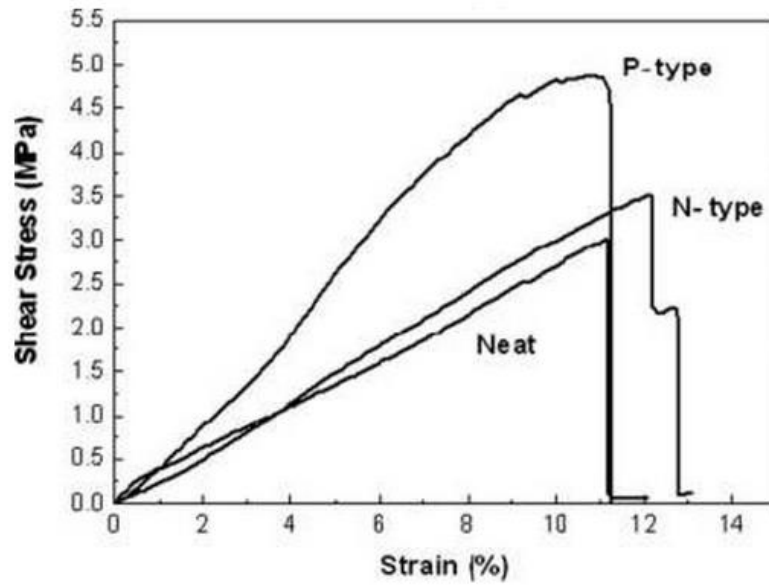


Figure 8: Shear stress-strain curves for syntactic foams (density = 250kg/m³).

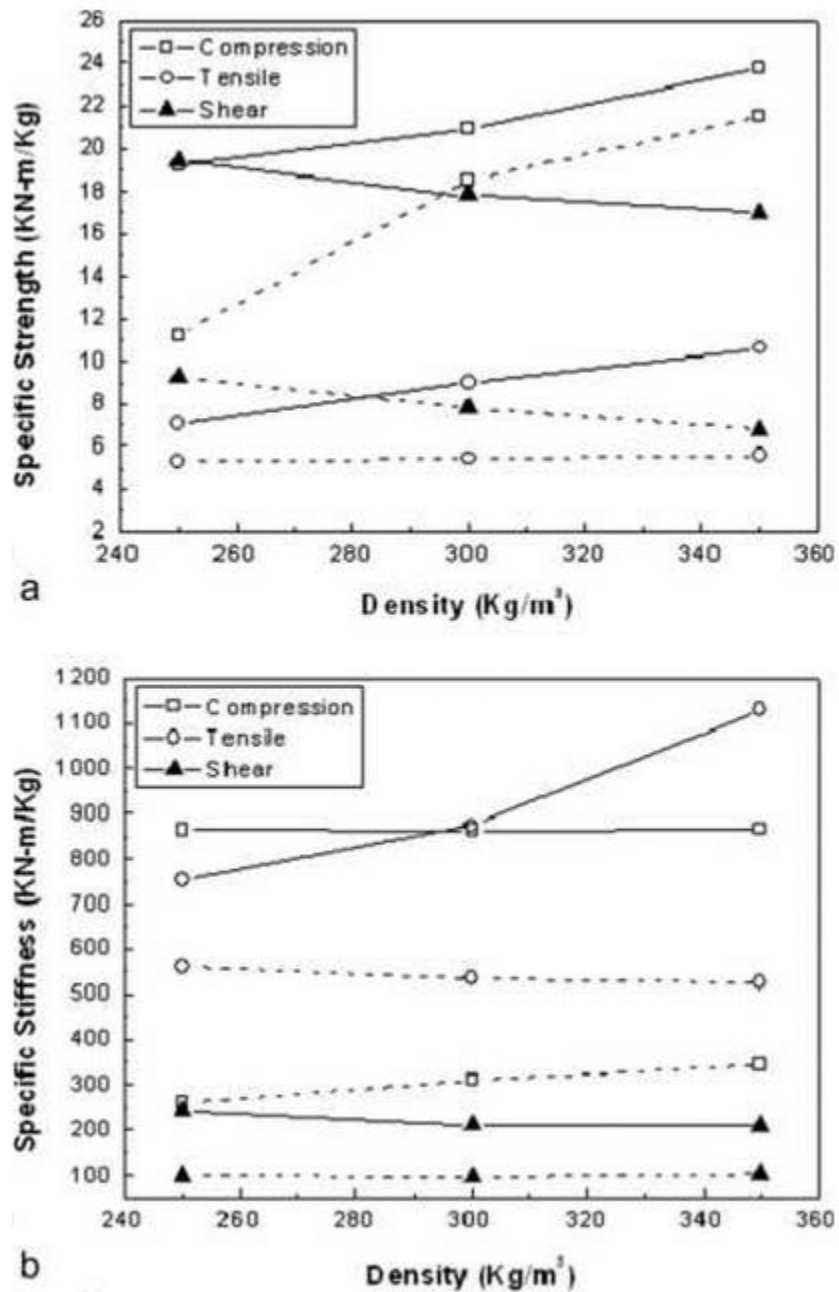


Figure 9: Specific strength and specific stiffness for the P-type foams and the neat foams. The bold solid lines are the lines for the P-type foam and the dash lines are the lines for the neat foams.



4. Conclusions

Composite syntactic foams composed of phenolic resin microspheres were fabricated with a small addition of chopped carbon fiber. Compressive, tensile, and shear properties of foams with different fiber orientations and densities were evaluated. The experimental results lead to several conclusions. Syntactic foams can be substantially strengthened by relatively small additions of short carbon fibers (i.e., 4 wt %), and the property enhancements are largely dependent on fiber orientation and foam density. Composite foams with fiber layer planes parallel to the loading direction (P-type) demonstrated significant improvements in specific properties in compression, tension, and shear. Fiber orientation is critical for fiber-reinforced syntactic foams, as it is for composite laminates. Over the density range examined, the relationship of foam properties to foam density exhibited power law behavior, albeit with different exponents.

Syntactic foams reinforced with other fibers (e.g., glass fiber, aramid fiber, etc.) are expected to exhibit similar enhancements in specific strength and specific modulus. Different reinforcing fibers should allow one to tailor property enhancements, by exploiting the specific fiber properties and their distribution in the matrix. For example, more flexible fibers should permit more random orientations, and thus the property enhancement could be less anisotropic. Reinforcing syntactic foams with fibers provides effective strengthening and toughening of the foams. Furthermore, interlacing of the fibers can enhance isotropic toughness through crack bridging and deflection. Efficient load transfer may make it possible to reduce the amount of resinous binding material, thereby reducing composite density while retaining high strength and high modulus. Fiber reinforcement affords enhancements in strength, stiffness, and toughness that are difficult or impossible through traditional methods such as changing the type, concentration, size, and wall thickness of micro-spheres, or modifying the



interface between the micro-spheres and the binding material. In terms of practical relevance, fiber reinforcement also enhances core-skin adhesion in sandwich structures, while elevating core properties to ranges comparable with those of honeycomb cores.

Acknowledgements: The authors also acknowledge Asia Pacific Micro-spheres Corp. for providing PHENOSET1 microspheres.

References:

1. A.H. Landrock, Handbook of Plastic Foams, Noyes Publications, New Jersey, 455 (1995).
2. D. Klemmner and V. Sendjarevic, Handbook of Polymeric Foams and Foam Technology, Hanser Gardener [i.e. Gardner] Publications, Cincinnati, **355**, 489 (2004).
3. C.S. Karthikeyan, S. Sankaran, and Kishore, Polym. Int., **49**,158 (2000).
4. M. Narkis, S. Kenig, and M. Puterman, Polym. Compos., **5**,159 (1984).
5. N. Gupta, Kishore, E. Woldesenbet, and S. Sankaran, J.Mater. Sci., **36**, 4485 (2001).
6. N. Gupta, E. Woldesenbet, and Kishore, J. Mater. Sci., **37**,3199 (2002).
7. H.S. Kim and H.H. Oh, J. Appl. Polym. Sci., **76**, 1324(2000).
8. N. Gupta, E. Woldesenbet, and P. Mensah, Compos. A, **35**,103 (2004).
9. P. Bunn and J.T. Mottram, Composites, **24**, 565 (1993).
10. N. Gupta, Kishore, S. Sankaran, and C.V. Raman Nagar, J.of Reinforced Plast. Compos., **18**, 1347 (1999).
11. N.N. Jize, C. Hiel, and O. Ishai, Compos. Mater., **12**, 125(1996).
12. C. Hiel, D. Dittman, and O. Ishai, Composites, **24**, 447(1993).
13. E. Woldesenbet, N. Gupta, and D.H. Jerro, J. Sandwich Struct. Mater., **7**, 95 (2005).
14. E. Wouterson, F. Boey, X. Hu, and S. Wong, Compos. Sci.Technol., **65**, 1840 (2005).
15. Kishore, R. Shankar, and S. Sankaran, J. Appl. Polym. Sci,**98**, 687 (2005).
16. N. Gupta, E. Woldesenbet, Kishore, and S. Sankaran,J. Sandwich Struct. Mater., **4**, 249 (2002).
17. C.S. Karthikeyan, S. Sankaran, M.N.J. Kumar, and Kishore,J. Appl. Polym. Sci., **81**, 405 (2001).
18. N. Gupta, C.S. Karthikeyan, S. Sankaran, and Kishore,Mater. Character., **43**, 271 (1999).
19. C.S. Karthikeyan, C.R.L. Murthy, S. Sankaran, and Kishore,Bull. Mater. Sci., **22**, 811 (1999).
20. E. Lawrence and R. Pyrz, Polym. Compos., **94**, 227 (2001).
21. Y. Huang, L. Vaikhanski, and S. Nutt, Compos. A, **37**, 48, (2006).
22. Technical information, Asia Pacific Corp. (2003).
23. Technical information, SGL Carbon AG (2003).
24. L.J. Gibson and M.F. Ashby, Cellular Solids, Structure and Properties, Cambridge University Press, Cambridge (1997).
25. A. Kelly, R. Cahn, and M. Bever, Concise Encyclopedia of Composite Materials, MIT Press Cambridge, Massachusetts, 1 (1994).
26. A.R. Luxmoore and D.R.J. Owen, Mechanics of Cellular Plastics, Applied Science Publishers, London, 359 (1982).
27. Masud and K.B. Zaman, J. Mater. Process. Technol., **172**, 258 (2006).